PAPER

Artificial neural networks and phenomenological degradation models for fatigue damage tracking and life prediction in laser induced graphene interlayered fiberglass composites

IOP Publishing Smart Materials and Structures
Smart Mater. Struct. **30** (2021) 085010 (15pp) https://doi.org/10.1088/1361-665X/ac093d

Artificial neural networks and phenomenological degradation models for fatigue damage tracking and life prediction in laser induced graphene interlayered fiberglass composites

Jalal Nasser[1], **LoriAnne Groo**[1] and **Henry Sodano**[1,2,3,*]

[1] Department of Aerospace Engineering, University of Michigan, Ann Arbor, MI 48109, United States of America
[2] Department of Macromolecular Science and Engineering, University of Michigan, Ann Arbor, MI 48109, United States of America
[3] Department of Materials Science and Engineering, University of Michigan, Ann Arbor, MI 48109, United States of America

E-mail: hsodano@umich.edu

Received 16 April 2021, revised 3 June 2021
Accepted for publication 7 June 2021
Published 22 June 2021

Abstract

The mechanical properties of fiber reinforced polymer matrix composites are known to gradually deteriorate as fatigue damage accumulates under cyclic loading conditions. While the steady degradation in elastic stiffness throughout fatigue life is a well-established and studied concept, it remains difficult to continuously monitor such structural changes during the service life of many dynamic engineering systems where composite materials are subjected to random and unexpected loading conditions. Recently, laser induced graphene (LIG) has been demonstrated to be a reliable, *in-situ* strain sensing and damage detection component in fiberglass composites under both quasi-static and dynamic loading conditions. This work investigates the potential of exploiting the piezoresistive properties of LIG interlayered fiberglass composites in order to formulate cumulative damage parameters and predict both damage progression and fatigue life using artificial neural networks (ANNs) and conventional phenomenological models. The LIG interlayered fiberglass composites are subjected to tension–tension fatigue loading, while changes in their elastic stiffness and electrical resistance are monitored through passive measurements. Damage parameters that are defined according to changes in electrical resistance are found to be capable of accurately describing damage progression in LIG interlayered fiberglass composites throughout fatigue life, as they display similar trends to those based on changes in elastic stiffness. These damage parameters are then exploited for predicting the fatigue life and future damage state of fiberglass composites using both trained ANNs and phenomenological degradation and accumulation models in both specimen-to-specimen and cycle-to-cycle schemes. When used in a specimen-to-specimen scheme, the predictions of a two-layer Bayesian regularized ANN with 40 neurons in each layer are found to be at least 60% more accurate than those of phenomenological degradation models,

* Author to whom any correspondence should be addressed.

displaying R^2 values greater than 0.98 and root mean square error (RMSE) values smaller than 10^{-3}. A two-layer Bayesian regularized ANN with 25 neurons in each layer is also found to yield accurate predictions when used in a cycle-to-cycle scheme, displaying R^2 values greater than 0.99 and RMSE values smaller than 2×10^{-4} once more than 30% of the initial measurements are used as inputs. The final results confirm that piezoresistive LIG interlayers are a promising tool for achieving accurate and continuous fatigue life predictions in multifunctional composite structures, specifically when coupled with machine learning algorithms such as ANNs.

Supplementary material for this article is available online

Keywords: laser induced graphene, fiberglass composites, fatigue life prognosis, artificial neural networks, phenomenological models

(Some figures may appear in color only in the online journal)

1. Introduction

Owing to their exceptionally high specific strength and stiffness, fiber reinforced composite materials have been increasingly integrated into large scale structural applications within the aerospace, automotive, and construction industries [1–3]. Given the critical nature of these applications, it is imperative to monitor and track the structural health of composite materials while in service in order to ultimately avoid sudden catastrophic failure [4, 5]. However, due to their heterogeneity, fiber reinforced composites are known to exhibit complex damage mechanisms throughout their service lives which incorporate various failure modes, primarily matrix cracking, fiber-matrix debonding, delamination, and fiber breakage [6]. As a result, numerous research efforts focused on incorporating functional elements within composite structures in order to detect and track these various forms of damage *in-situ*, yielding structural health monitoring (SHM) techniques such as acoustic emission testing [7–9], embedded fiber optics [10, 11], and electrical impedance-based methods [12, 13]. Yet many of these methods typically result in trade-offs between the newly integrated self-sensing functionality and the final mechanical performance of these composite materials. Therefore, optimal SHM methods are required to enable strain sensing and damage detection in composite materials while avoiding any deterioration to their mechanical properties.

Over the years, piezoresistivity-based methods have continuously garnered great interest within the SHM research community due to their relative simplicity, their ease of implementation, and their compatibility with a wide range of composite materials. Initial work focused on exploiting the inherent peizoresistivity of carbon fibers to detect and monitor structural damage within their corresponding composites *in-situ* [14–16]. Specifically, the changes in the electrical resistance of carbon fiber composites during cyclic loading were correlated to fatigue life and then used to formulate fatigue life prediction guidelines [16]. However, such an approach was found to be considerably less sensitive to more critical damage modes that occur earlier during fatigue life, such as matrix cracking and delamination, which is expected when relying on the reinforcing carbon fiber phase to act as a damage sensor. Additionally, the described method remains exclusively restricted to composite materials that use conductive reinforcing components, such as carbon fibers. Nonetheless, the continuous growth of the nanomaterials field has enabled the incorporation of electrically conductive nanofillers, such as carbon black [17, 18] and carbon nanotubes (CNTs) [12, 19, 20] into electrically insulating composite materials for embedding a self-sensing functionality. Particularly, the excellent mechanical and electrical properties of CNTs have made them a strong candidate for tracking damage progression in fiberglass composites under cycling loading conditions [21, 22]. Efforts by Gao *et al* clearly demonstrated the ability of CNTs to distinguish between various damage mechanisms that occur under cyclic loading such as crack initiation, transverse micro-cracking, and delamination [23]. Yet CNTs still present considerable processing and fabrication challenges due to their tendency to agglomerate when being mixed in epoxy resins [24, 25] or due to them requiring harsh thermal and chemical growth conditions when grown on fiber surfaces [26, 27]. More recently, the embedding of laser induced graphene (LIG) interlayers have been demonstrated as a reliable and successful approach for the fabrication of multifunctional aramid and fiberglass composite materials [28–31]. The simple and cost-effective LIG fabrication process [32, 33] was successfully exploited by Groo *et al* to embed LIG interlayers within fiberglass composites and enable *in-situ* strain sensing, damage detection and localization, and failure mode classification. Furthermore, the piezoresistive LIG interlayers were found capable of tracking matrix-cracking, delamination, and fiber failure in fiberglass composites throughout their fatigue life [34]. However, the described work lacks any extensive investigation of the damage evolution and accumulation mechanisms that can be potentially discerned by the LIG interlayers, thus hindering the realization of accurate fatigue life predictions in fiberglass composite materials using such a technique.

The prediction of fatigue life in composite materials have been typically achieved through either mechanical [35, 36] or phenomenological damage models [37]. While the former can provide more accurate predictions than the latter, the

reliability of mechanical damage models, such as Owen and Howe [38] or Palmgren–Miner [39], is typically limited in application by their material- and condition-specificity, which require a considerable amount of empirical characterization experiments and complex mechanical analysis. On the other hand, phenomenological models aim to describe the fatigue behavior of composite materials by capturing the evolution and changes in their macroscopic properties, primarily the loss of material strength or stiffness due to damage accumulation. While both strength and stiffness degradation models have been developed, stiffness models have attracted greater research interest due to the considerably lesser degree of scatter in collected residual stiffness measurements relative to that of residual strength [40]. As a result, numerous linear and non-linear stiffness degradation models have been formulated and used to provide accurate fatigue life predictions [40–45]. More recently, artificial intelligence (AI) technologies such as neural networks (NNs) have emerged as a reliable tool for predicting the mechanical behavior and response of a variety of structural materials, such as metals [46, 47] and fiber reinforced composites [48–50], in a wide range of applications. The advantages of these NN methods over conventional models lie in their superior extrapolation accuracy, their material and mechanism independence, and their ability to provide new insights into the examined response which conventional models are typically unable to reveal [51–53]. Recent work has shown that NNs can be used for predicting stiffness degradation in composite materials during fatigue through time-series forecasting approaches. For example, Tao *et al* reported a new NN architecture that relies on a combination of a β-variational autoencoder and neural ordinary differential equations to continuously and accurately predict the stiffness response of composite materials over the cycle domain [54]. Nonetheless, all stiffness degradation models remain hindered by the difficulty of directly obtaining stiffness reduction measurements while a composite structure is in service. Therefore, it is desirable to infer these changes to the elastic stiffness of composite materials using one or more of the currently established SHM techniques. Zhang *et al* proposed a new method that relies on the mode conversion behavior of guided waves to quantify changes in the mechanical properties of fiberglass composites under cyclic loading [55], while Peng *et al* developed a real-time composite fatigue life prognosis framework that estimates changes in stiffness using a Lamb wave-based damage detection method [56]. Elsewhere, Seo *et al* demonstrated that piezoresistive measurements can also be correlated to stiffness reduction during the fatigue life of carbon fiber composites, and then used these measurements to predict future stiffness degradation behavior, and ultimately fatigue failure [57]. Such results highlight the potential for coupling resistance-based SHM methods with stiffness degradation models in order to accurately predict fatigue life and damage accumulation behavior in composite materials during service.

In this work, the piezoresistive response of LIG interlayered fiberglass composites was investigated in order to formulate cumulative fatigue damage parameters and predict both fatigue life and future damage progression in fiberglass composite materials. The LIG interlayers were transfer-printed from polyimide substrates to fiberglass prepreg surfaces before subjecting the cured fiberglass composites to tension–tension fatigue testing. Changes in both the electrical resistance and elastic stiffness of the fiberglass specimens were passively monitored throughout fatigue life up until failure. The observed trends in elastic stiffness and electrical resistance response were then compared and used to define cumulative damage parameters for fatigue life predictions using both artificial neural networks (ANNs) and phenomenological degradation and accumulation models. Finally, the fatigue damage predictive potential and capabilities of these ANNs and conventional phenomenological models when relying on the piezoresistive response of the LIG interlayers were compared and evaluated.

2. Materials and methods

2.1. LIG transfer and composite fabrication

Uniform LIG interlayers were introduced on the surface of fiberglass prepregs using the simple transfer printing process previously described by Nasser *et al* [58]. Initially, vertically aligned arrays of LIG were directly generated on a commercial polyimide film (0.0254 mm thick Kapton® tape sheets) using a 40 W CO_2 infrared laser (Epilog Zing 16 universal laser system) that was operated in raster mode at a pulsing density of 400 DPI, laser output power of 16%, and a raster speed of 1 cm^2 s^{-1}. The described laser induction parameters have been previously shown to be optimal for successfully transferring uniform and electrically conductive LIG interlayers onto fiberglass prepreg composites, while maintaining their excellent mechanical properties [30, 59]. The LIG interlayer was then transferred from the irradiated polyimide tape to the surface of uncured fiberglass prepregs (CYCOM® E773 epoxy prepreg with S-2 glass fiber-reinforced roving) [60] using a transfer printing process where the prepreg is rolled across the 80 °C pre-heated polyimide substrate while applying manual pressure. Once the transfer-printing process was successfully completed, the LIG interlayered fiberglass prepregs were combined in a (+45°/−45°/+45°) stacking sequence and cured at 127 °C under vacuum in a hot press and at a constant pressure of 100 psi (689.5 kPa). Specimens were then cut from the fabricated laminate to dimensions of 10 mm in width and 76 mm in length for subsequent mechanical testing. In order to avoid slippage and provide insulation between the specimens and the electrically conductive metallic grips, fiberglass tabs were adhered to the end of the specimens using high shear strength epoxy (Loctite® 9430™ Hysol®). Thin lines of silver paint were then added around the edges of the specimens at each end in order to act as electrodes during fatigue testing. The described sample configuration allows for electrical resistance measurements across the entire specimen rather than just at the LIG interlayer located along the top ply. Finally, copper wires were attached to each electrode using additional silver paint and epoxy which keeps them fixed during dynamic testing. For reference, the final electrical resistances of the fabricated specimens were measured to range between 200 and 900 Ω.

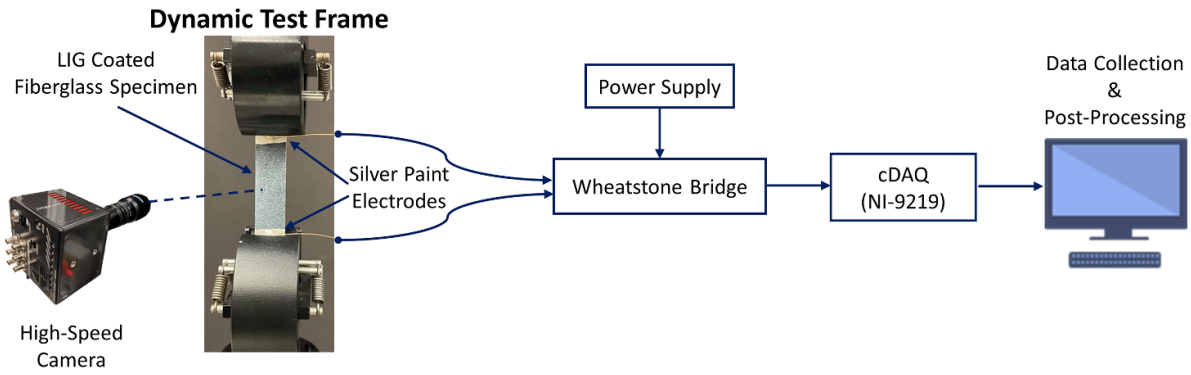

Figure 1. Schematic of experimental fatigue testing setup.

2.2. Dynamic testing and resistance measurements

Initially, quasi-static tensile testing was performed according to ASTM D3039 on an Instron model 5982 test frame using a 100 kN load cell. Once the average ultimate strength (σ_{ult}) and initial elastic stiffness (E_0) of the LIG interlayered fiberglass specimens were determined, 13 additional samples were subjected to load-controlled tension–tension fatigue testing using an Instron ElectroPuls^{TM} model E1000 loading frame equipped with a ± 1 kN load cell (Figure 1). The tests consisted of 10 Hz sine wave excitation at a stress ratio R of 0.1 ($R = \sigma_{min}/\sigma_{max}$) and maximum stress levels that ranged between 65% and 78% of σ_{ult}. The decrease in the elastic stiffness of the specimens was monitored throughout fatigue life directly using the dynamic test frame. Concurrently, the changes in the electrical resistance of the specimens were measured using a traditional Wheatstone bridge circuit, where input voltage was provided using a Hewlett Packard model 6217A DC power supply, while output voltage was recorded using a National Instrument compact data acquisition system. The recorded resistance measurements were averaged every one second, which corresponded to one measurement point for every 10 tension–tension loading cycles. It should be noted that the accumulation in damage throughout fatigue life was also monitored using digital imaging correlation (DIC) and analysis of the speckled fiberglass specimen surfaces, which was achieved using a Photron FASTCAM Mini AX 200 high-speed camera operating in periodic bursts at 1000 frames per second. The initial mechanical and electrical properties of the LIG interlayered fiberglass specimens are shown in table 1.

Table 1. Properties of $(+45^\circ/-45^\circ/+45^\circ)$ LIG coated fiberglass laminate.

Laminate properties
Nominal ply thickness = 0.21 mm
$v_f = 0.55$
$\sigma_{ult} = 109.65$ MPa
$E_0 = 23.45$ GPa
$R_0 = 200$–$900\ \Omega$

2.3. Artificial neural network (ANN) design

ANNs are machine learning algorithms that are designed to simulate the functioning principles of a brain by automatically and independently learning from large sets of data, processing them, inferring relationships and patterns, and ultimately generalize these learning outcomes for future decision making [61]. The fundamental element of these ANNs are termed neurons, which are the processing units enabling communication between the various layers of the network, namely, the input, hidden, and output layers. As described in Kara *et al*, the net input of each neuron is typically obtained using a summation function that combines the various input activations into a single one, while also applying weights and biases [47]. The net weighted sum of the input into to the ith neuron (NET_i) is then processed through an activation function that determines the output of the neuron, and ultimately dictates the overall performance of the network. Due to their wide use as activation functions in ANNs, both sigmoid and hyperbolic tangent (tanh) functions were considered in this work. However, given its superior performance and faster convergence rate, an asymmetric tanh function was preferred over a sigmoid one for the choice of logistic transfer function in this work, such as:

$$f(\mathrm{NET}_i) = \frac{e^{\mathrm{NET}_i} - e^{-\mathrm{NET}_i}}{e^{\mathrm{NET}_i} + e^{-\mathrm{NET}_i}} \tag{1}$$

where f is a rescaling of the logistic sigmoid function in order to yield an output that ranges between -1 and 1. Additionally, the design of the ANN architecture requires determining the optimal learning algorithm, number of hidden layers, and the number of neurons in each one of these layers. Different ANN training algorithms were investigated in this work, such as quasi-Newton backpropagation (BFGS), Levenberg–Marquardt backpropagation (LM), scaled conjugate gradient backpropagation, resilient backpropagation, and Bayesian regulation backpropagation (BR). In this case, only LM, BFGS, and BR were found to yield suitable fatigue damage and remaining life predictions, with BR outperforming the other two training algorithms (table S1 (available online at stacks.iop.org/SMS/30/085010/mmedia)). This is expected given that BR training algorithms have been shown to

enable more robust models that are capable of capturing complex and non-linear relationships [62]. Additional ANN design parameters pertaining to these learning algorithms are also provided in table S2. It should also be noted that the coupling of these training algorithms with two hidden layers instead of one was found to improve error convergence in these ANN networks. When aiming to perform predictions based on specimen-to-specimen and cycle-to-cycle schemes, the optimal ANN architectures were found to consist of 40 and 25 neurons in each hidden layer, respectively. The experimental data consisted of the electrical resistance response of the LIG interlayered fiberglass specimens and their corresponding normalized fatigue cycles, which were randomly split between training and testing cases at a ratio of ∼75:25 for both of the previously mentioned prediction schemes. Finally, the performance of the ANN models was assessed by comparing their predictions to the experimental results through calculating the root mean square error (RMSE) and the coefficient of correlation (R^2), such that:

$$\mathrm{RMSE} = \left(\left(\frac{1}{p} \right) \sum_j |t_j - o_j|^2 \right)^{1/2} \tag{2}$$

$$R^2 = 1 - \left(\frac{\sum_j (t_j - o_j)^2}{\sum_j (o_j^2)} \right) \tag{3}$$

where t represents the goal values, o the output values, and p is the number of samples.

3. Results and discussion

3.1. Predictions using phenomenological models

Under cyclic loading conditions, composite materials are expected to experience non-linear progression in damage prior to catastrophic structural failure. Phenomenological models aim to describe and quantify such damage through macroscopic parameters, such as material strength or stiffness. As seen in figure 2(A), these material properties will exhibit progressive degradation throughout fatigue life which can be divided into three distinct phases [42, 63]. Initially, the degradation process is dominated by matrix cracking and material relaxation, before stabilizing in the form of a steady and gradual decrease due to a combination of delamination and fiber-matrix debonding. Finally, the last stage consists of a sudden and abrupt increase in degradation rate due to fiber failure and delamination, which ultimately leads to quick and near-immediate catastrophic failure. Therefore, these various forms of damage and mechanisms can be captured and described by monitoring the degradation in the elastic stiffness of composite materials. Given that fatigue testing here is performed in a load control mode and at a fixed stress ratio of $R = 0.1$, the elastic stiffness of the LIG interlayered fiberglass composites is expected to decrease with increasing number of loading cycles, thus yielding an increase in strain (figure 2(B)). It should be noted that under the described conditions, the stiffness degradation rate is expected to be strictly a function of $\sigma_{\max}$, E_0, and R. Based on the stiffness degradation damage parameter (D_{E}) defined in figure 2(B), the reduction in elastic stiffness throughout the fatigue life of the LIG interlayered fiberglass specimens is found to be in good agreement with the general trend shown in figure 2(A). Similarly, a new damage parameter can be defined to express changes in the electrical resistance (D_{R}) of LIG interlayered fiberglass specimens. Recently, Groo *et al* demonstrated the capability to use these piezoresistive interlayers to track various damage modes throughout the fatigue life of fiberglass composites, while showing good agreement between the obtained trends in measured strain and electrical resistance [34]. Since elastic stiffness is inversely proportional to strain, the damage parameter D_{R} is here defined to be inversely dependent on the electrical resistance of the specimens. Such a definition yields a D_{R} trend that is in good agreement with the general trend seen in figure 2(A), especially during the second and third damage phases (figure 2(C)). When examining figure 2(D), which shows D_{E} and D_{R} for a representative specimen, both damage parameters display comparable trends throughout fatigue life, in addition to being sensitive to the various damage phases experienced by the fiberglass specimen. Therefore, the piezoresistive response of the LIG interlayer can be potentially integrated with pre-existing stiffness degradation models in order to provide *in-situ* damage and fatigue life prognosis of fiberglass composite materials.

Using the stiffness degradation model suggested by Yang *et al* [43, 64, 65], the electrical resistance damage parameter, D_{R}, shown in figure 2 can be used to predict the future damage state of fiberglass composite materials. The proposed model assumes the rate of change in D_{R} to be a power function of the number of load cycles, yielding the following relationship:

$$D_{\mathrm{R}}(n) = 1 - Qn^{v} \tag{4}$$

where n is the number of cycles, while Q and v are material constants that can be determined using a least-square fitting. For brevity, the predicted and experimental D_{R} of only two LIG interlayered fiberglass specimens are shown in figure 3. When comparing the predicted results to the experimental ones, it is clear that the obtained predictions using the model suggested by Yang *et al* are in good agreement with the experimental results, especially during the first two stages of fatigue life. However, as expected, the model fails to accurately predict the final failure stage of fiber breaking, due to the abrupt and highly non-linear change in the trend of D_{R} which cannot be accurately modeled by a power function. Nonetheless, these results confirm the capability of predicting future damage in fiberglass composites within the earlier stages of fatigue life and at various stress levels by solely relying on the piezoresistive response of the LIG interlayers embedded in them.

In the case where no prior base-line data is available, initial electrical resistance measurements can be used to accurately forecast future damage in LIG interlayered fiberglass composites based on a cycle-to-cycle scheme. By assuming that $Q(k)$ and $v(k)$ are the best estimates of material constants Q and v at cycle n_k, boundary conditions can be applied to equation (4),

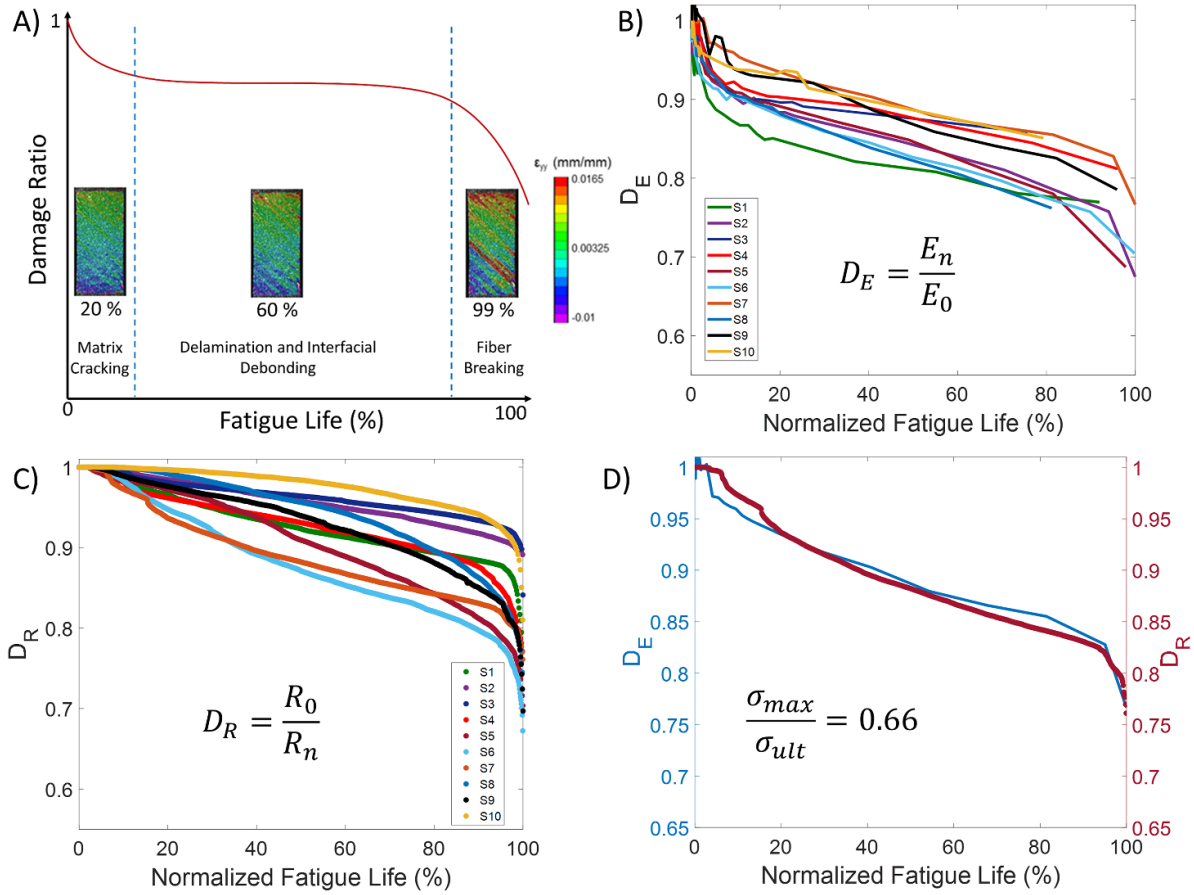

Figure 2. (A) General trend for stiffness degradation in composite materials throughout fatigue life and corresponding DIC images for each damage phase. (B) Reduction in elastic stiffness (D_E) of LIG interlayered fiberglass composites throughout fatigue life and at different stress levels, where E_0 and E_n represent the elastic stiffness at cycles 0 and n of the fatigue life, respectively. (C) Reduction in electrical resistance damage parameter (D_R) of LIG interlayered fiberglass composites throughout fatigue life and at different stress levels, where R_0 and R_n represent the electrical resistance at cycles 0 and n of the fatigue life, respectively. (D) Elastic stiffness and electrical resistance damage parameters of a $(+45^\circ/-45^\circ/+45^\circ)$ specimen throughout fatigue life (S7).

such as $D_R(n) = D_R(n_k)$, and the following relationship can be obtained:

$$Q(k) = \frac{1 - D_R(n_k)}{(n_k)^{v(k)}}. \tag{5}$$

Which can be then re-substituted in equation (4) and transformed into a linear regression formulation for obtaining $v(k)$ such as:

$$\ln\left(\frac{D_R(n)}{D_R(n_k)}\right) = v(k)\ln\left(\frac{n}{n_k}\right). \tag{6}$$

Once $v(k)$ and $Q(k)$ are estimated, future values of D_R can be predicted for the remaining life cycles. Additionally, the values of both constants can be continuously updated with both increasing number of elapsed cycles and recorded electrical resistance measurements in order to further improve the accuracy of these predictions. A comparison between the experimental and predicted electrical resistance damage response of two LIG coated fiberglass specimens based on a cycle-to-cycle scheme is shown in figures 4(A) and (B). As expected, the prediction accuracy is improved with an increasing number of initial observations, as the model displays good agreement with experimental results once more than 30% of the electrical resistance measurements become available. Such results indicate that D_R can be used to accurately predict future damage in fiberglass composites without requiring extensive experimental characterization prior to its use. Nonetheless, the used model remains incapable of fully predicting the fatigue life of fiberglass composites due to its inability to capture the final damage phase of fiber breakage. Yang *et al* formulated a criterion that allows for fatigue life predictions using the proposed model, where stiffness at failure (E_f) is defined to be linearly dependent on the $\sigma_{max}/\sigma_{ultimate}$ ratio [65]. In a similar fashion, a linear relationship can be determined to describe the relationship between D_R at failure (R_0/R_f) and the $\sigma_{max}/\sigma_{ultimate}$ ratio, which can then be used to predict fatigue life (N_f). Nonetheless, the described approach is known to greatly overpredict fatigue life, which is undesirable in real life applications and can result in safety concerns [65]. Elsewhere, Suzuki *et al* demonstrated that incorporating an additional criterion for the determination of fatigue life during the final stage of

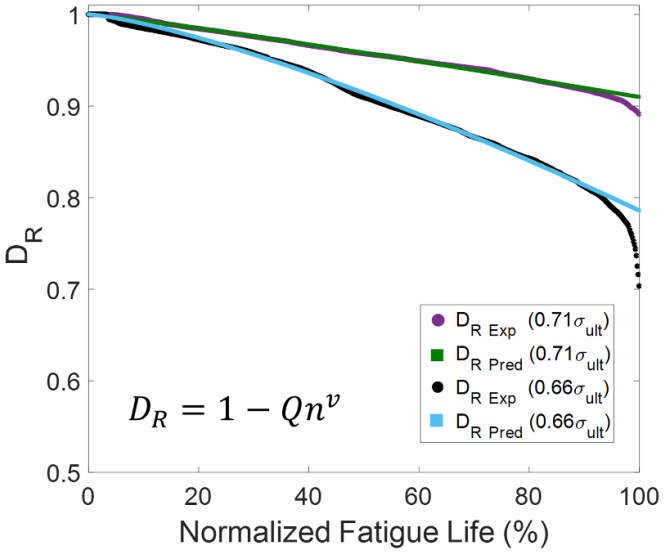

Figure 3. Comparison between predicted and experimental reduction in the electrical resistance damage parameter (D_R) of LIG interlayered fiberglass composites throughout fatigue life and at two different stress levels.

fiber failure, such that 100% of fatigue life is designated to be located at a degradation slope ($d/dN(D_R)) = -0.01$, can considerably improve fatigue life predictions [40]. Therefore, by combining these two criterions, fatigue life can be predicted according to the approach shown in figure 4(C). While the forecasted fatigue life is an under-prediction of the experimental one and is largely a representation of the transition from the second to the third damage phase, fiber breakage dominates less than 10% of the total fatigue life and usually occurs in the form of sudden catastrophic failure. Therefore, such under-predictions of fatigue life can potentially help avoid dealing with the uncertainties that take place during the final damage phase of composite materials when cyclically loaded. As observed in figure 4(D), predictions of N_f are improved with an increasing number of available fatigue cycles, reaching an error of less than 10% when more than 40% of the electrical resistance measurements become available. However, a disadvantage of the detailed prediction method lies in it requiring prior experimental characterization in order to define a linear fit between R_0/R_f and $\sigma_{max}/\sigma_{ultimate}$ ratios, which can be prone to large scattering and inaccuracies [64]. Additionally, a new linear fit is required for specimens of different E_0, thus necessitating an extensive amount of experimental characterization and limiting the applicability and scalability of this technique to a wide range of composite materials. Therefore, it is preferable to investigate other phenomenological models and approaches than can circumvent these issues and accurately describe the final damage phase occurring in composite materials.

Another form of phenomenological model focuses on studying the synchronous evolution and accumulation of damage in composite materials due to the degradation of their mechanical properties. As seen in figure 5(A), the amount of accumulated damage will progressively increase throughout fatigue life along the three previously discussed damage phases. Similarly, both the first and third phases of matrix cracking and fiber breakage, respectively, display a considerably faster rate of accumulation relative to the more stable second phase of delamination and fiber-matrix interfacial debonding. Such damage accumulation curves can be obtained through the definitions of new damage parameters, D_{EE} and D_{RR}, shown in figures 5(B) and (C), respectively. Here, the damage parameters are bound between 0, which indicates an undamaged specimen, and 1, which signifies complete catastrophic failure. Therefore, these defined parameters can accurately represent the continuous and gradual changes in the structural state of composite materials throughout the duration of their fatigue life. The trends in both D_{EE} and D_{RR} of LIG interlayered fiberglass specimens throughout fatigue life are found to be in good agreement with the general damage accumulation trend displayed in figure 5(A). It should be noted that, in this case, D_{RR} is defined to be directly proportional to the electrical resistance of the specimens in order to obtain similar trends to those of D_{EE}. When examining figure 5(D), both D_{EE} and D_{RR} show acceptable agreement with regards to their trends throughout fatigue life, in addition to being sensitive to the various damage phases experienced by the specimens during cyclic loading. Given these trends, damage accumulation phenomenological models can be explored for providing *in-situ* damage and fatigue life prognosis of fiberglass composite materials using the piezoresistive response of their embedded LIG interlayers.

A number of formulations have been suggested to model fatigue damage accumulation in composite materials using elastic stiffness measurements. Based on the previously discussed results, such models can be adjusted and applied to electrical resistance measurements provided by the LIG interlayers embedded within the fiberglass specimens. Here, two different numerical models are used to describe the non-linear evolution in damage across fatigue life, and the results are shown in figures 6(A) and (B). The Weibull cumulative density function proposed by Suzuki *et al* [40] can be adjusted to describe evolution in the electrical resistance damage parameter (D_{RR}) such as:

$$D_{RR}(n) = \gamma\left(\ln\frac{N_f}{n - N_f}\right)^k \tag{7}$$

where N_f is fatigue life, γ and k is are scale and shape parameter that can be both obtained through a least-square fitting, respectively. In addition, another non-linear damage evolution model was suggested by Wu *et al* [41]:

$$D_{RR}(n) = 1 - \left(1 - \left(\frac{n}{N_f}\right)^B\right)^A \tag{8}$$

where A and B are two material modeling parameters that can be obtained through a least-square fitting. The results of

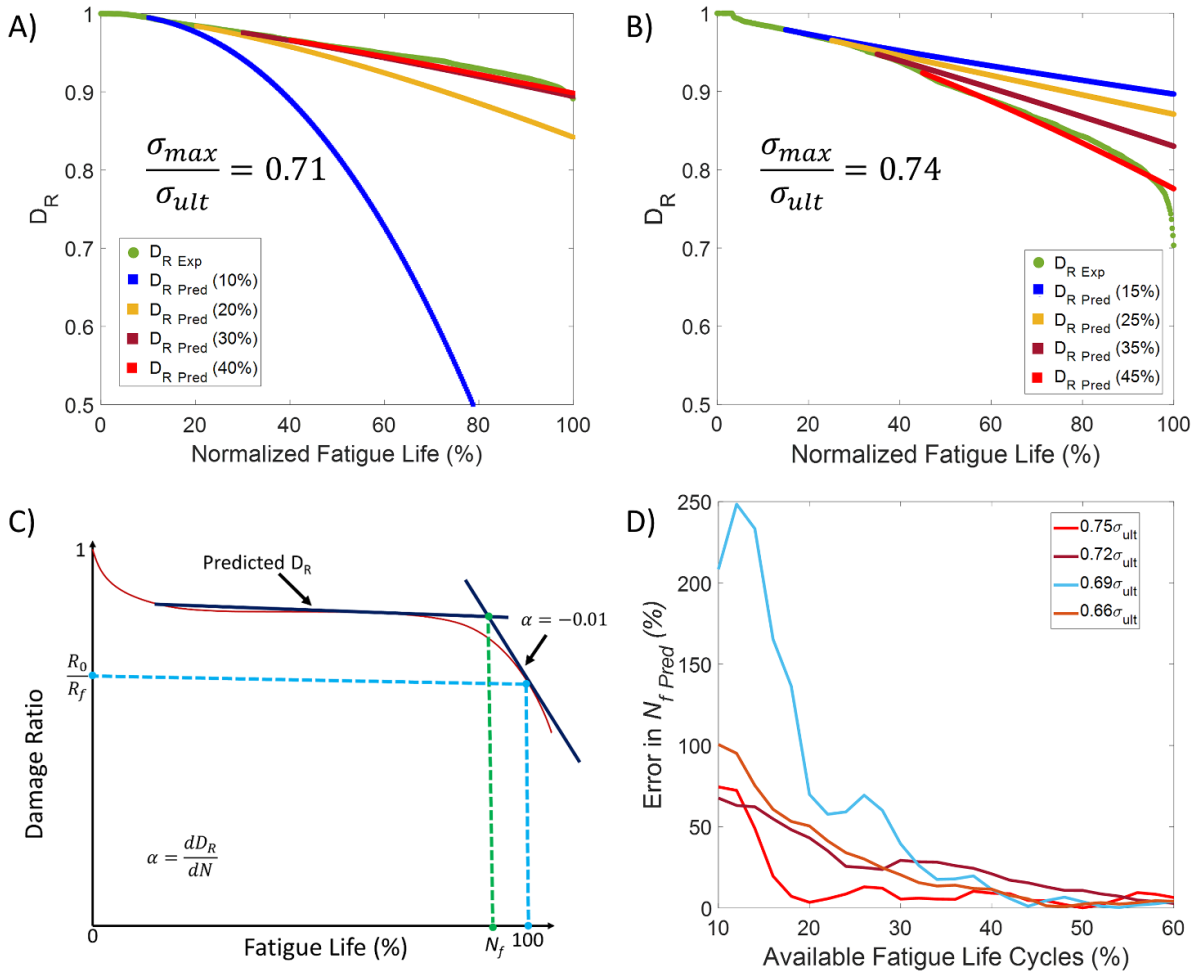

Figure 4. (A), (B) Phenomenological model predictions of the reduction in electrical resistance damage parameter (D_R) of LIG interlayered fiberglass composites according to a cycle-to-cycle scheme. (C) Criterion for fatigue life predictions using electrical resistance damage parameter (D_R) according to the change in degradation rate. (D) Error in fatigue life predictions ($N_{f\,Pred}$) with increasing number of available fatigue life cycles for LIG interlayered fiberglass composites at various stress levels.

both models can be seen in figures 6(A) and (B), where, for brevity, only the predicted and experimental D_{RR} of two LIG interlayered fiberglass specimens are shown. When comparing the performance of both models, the predicted results are found to be in relatively good agreement with the experimental ones during the last two phases of fatigue life. However, the first damage phase of matrix cracking is poorly represented by both models. Nonetheless, this is expected, as Groo *et al* observed that the increase in the electrical resistance of LIG interlayered fiberglass composites during the first damage phase of matrix cracking is considerably less pronounced than the increase occurring during the later stages of debonding, delamination, and fiber failure [34]. This was reasoned to be due to matrix cracking yielding considerably less physical separation within the LIG interlayer, and therefore having a significantly smaller effect on its piezoresistive response. Therefore, such models are unable to accurately predict changes in D_{RR} during the earlier cycles of fatigue life. Furthermore, while these models are capable of describing the final damage phase of fiber failure, prior knowledge of N_f is required, which necessitate extensive experimental characterization and restricts the use of such models in fatigue damage and life prediction frameworks that operate based on a cycle–cycle scheme. Similar shortcomings are also faced when using other suggested models, such as the one by Shiri *et al* which relies on trigonometric functions to describe damage accumulation in composite materials [45]. Therefore, despite phenomenological models providing insightful and accurate information regarding both material properties degradation and damage progression throughout the fatigue life of composite materials, it is important to explore more robust predictive methods that are capable of overcoming all the previously described limitations.

3.2. Predictions using ANNs

AI driven methods are considered to be a superior alternative to numerical modeling approaches due to their ability to address intractable and cumbersome problems whose analytical solutions are typically difficult to obtain, while also being, in this case, material- and mechanism-independent. Given the time-series forecasting nature of the degradation in

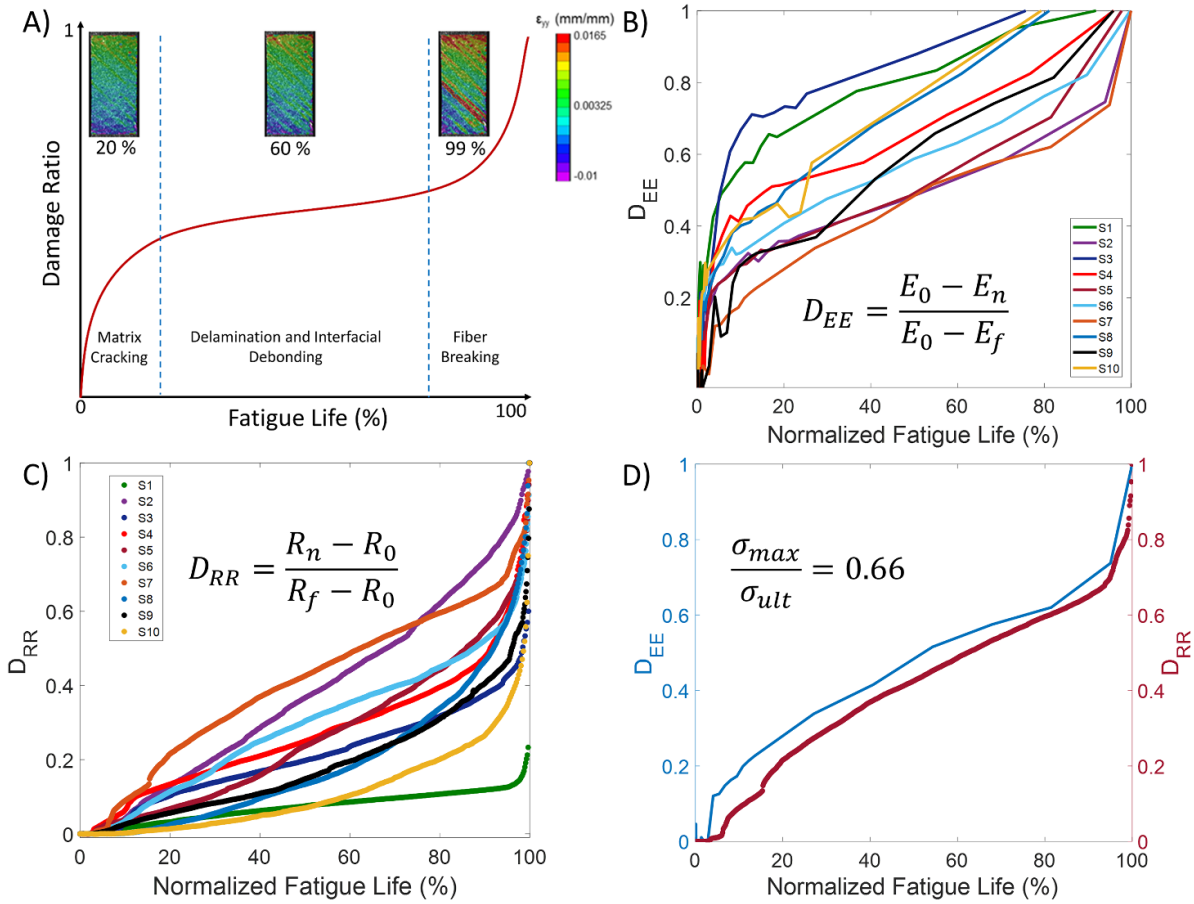

Figure 5. (A) General trend for damage evolution and accumulation in composite materials and corresponding DIC images for each damage phase. (B) Evolution in elastic stiffness damage accumulation (D_{EE}) throughout the fatigue life of LIG interlayered fiberglass composites at different stress levels, where E_0, E_n, E_f represent the elastic stiffness at cycles 0, n, and failure, respectively. (C) Evolution in electrical resistance damage accumulation parameter (D_{RR}) throughout the fatigue life of LIG interlayered fiberglass composites at different stress levels, where R_0, R_n, R_f represent the electrical resistance at cycles 0, n, and failure, respectively. (D) Elastic stiffness and electrical resistance damage parameter of a $(+45^\circ/-45^\circ/+45^\circ)$ specimen during fatigue loading (S7).

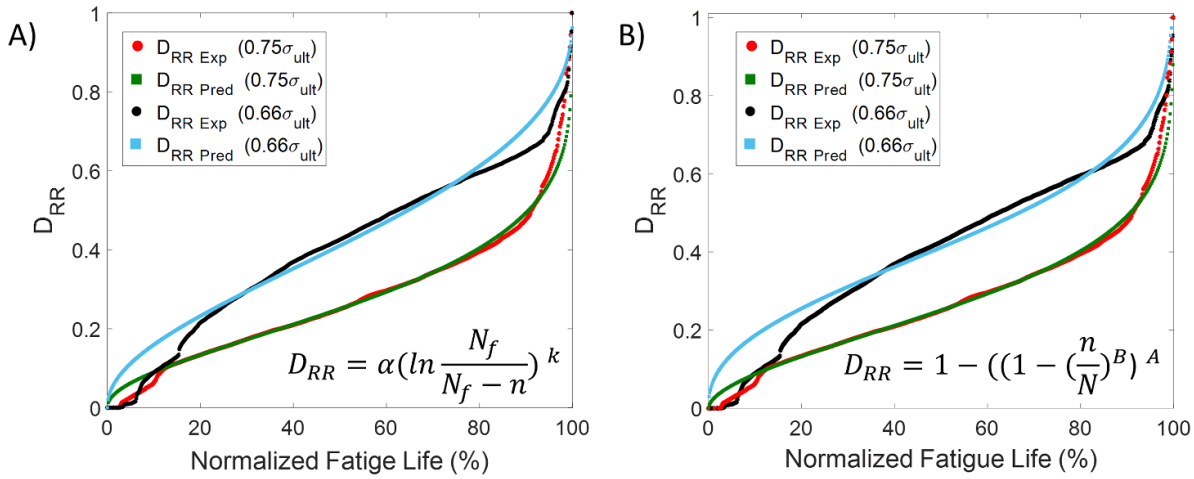

Figure 6. (A), (B) Comparisons between predicted and experimental changes in the electrical resistance damage accumulation parameter (D_{RR}) of LIG interlayered fiberglass composites throughout fatigue life using two different phenomenological accumulation models and at two different stress levels.

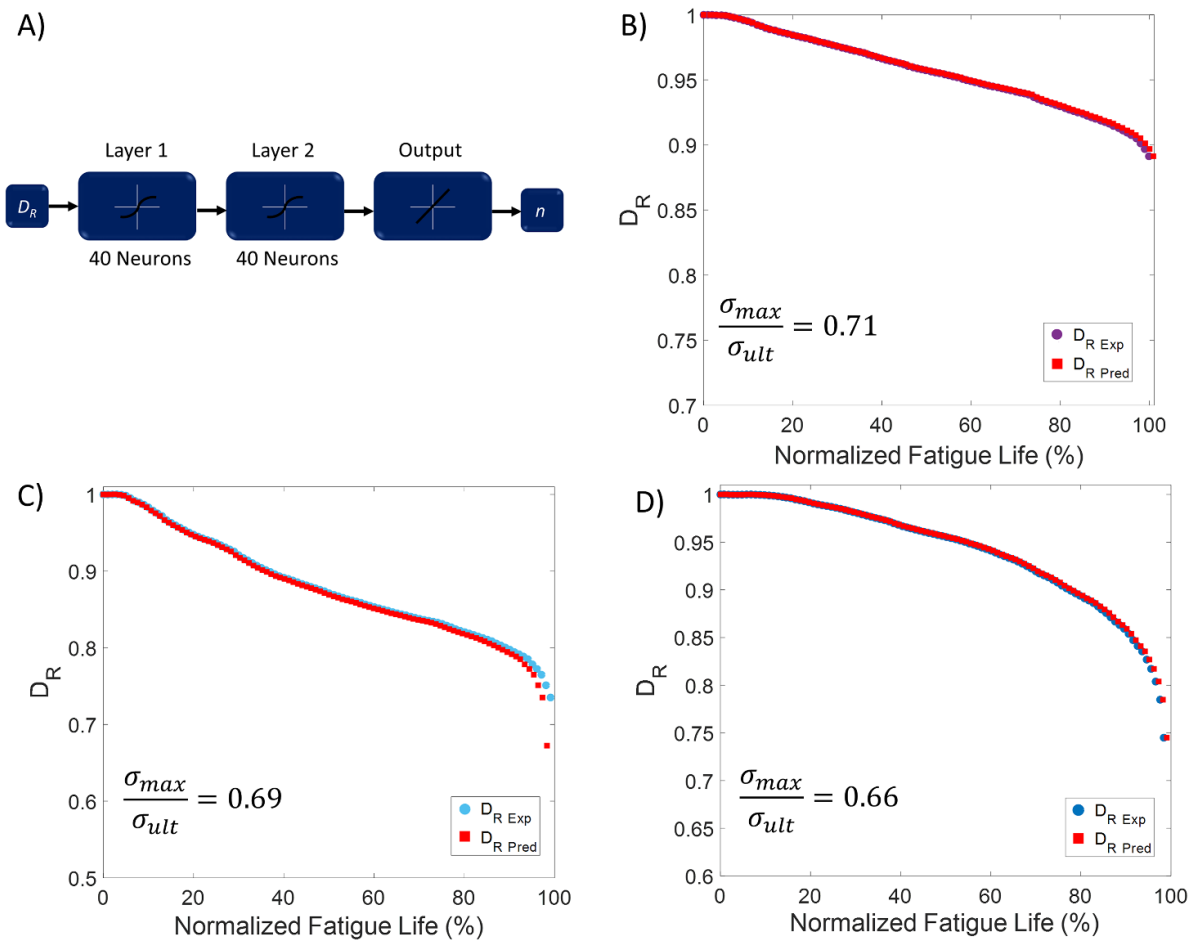

Figure 7. (A) Diagram of used two-layer Bayesian regularized ANN with an optimal number of 40 hidden units or neurons in each layer (ANN_1). (B)–(D) Comparisons between ANN predicted and experimental fatigue life cycles of LIG interlayered fiberglass composites based on the reduction in electrical resistance damage parameter (D_R) at three different stress levels.

the mechanical properties of composite materials throughout fatigue life, ANNs are expected to be the most suitable form of algorithms for continuously predicting fatigue damage and remaining life in the cycle domain [54]. Therefore, ANNs can be first trained to learn the underlying mechanisms behind the progressive degradation in elastic stiffness before then using them to potentially achieve more accurate predictions. However, instead of relying on a reduction in the elastic stiffness of the LIG interlayered fiberglass specimens, electrical resistance measurements can be used in the form of damage parameter D_R to describe damage progression. As previously detailed, D_R and D_E have been shown to be in good agreement throughout all the different fatigue damage phases of fiberglass composites. Furthermore, unlike D_{RR}, D_R does not require prior knowledge of the electrical resistance of the fiberglass specimens at failure (R_f), which eliminates the need for any additional assumptions and reduces prediction inaccuracies. Here, a two-layer Bayesian regularized ANN with an optimal number of 40 hidden units or neurons in each layer (ANN_1) is trained to learn the relationship between D_R and fatigue life and then predict fatigue damage in a new fiberglass specimen. It should be noted that the use of two hidden layers instead of one was found to improve error convergence, which is expected given that prediction accuracy is largely dependent on ANN architecture. The training of the ANN is achieved by providing the D_R of 10 LIG interlayered fiberglass specimens as inputs to the ANN, while using their corresponding fatigue cycles (n) as target outputs (figure 7(A)). In order to investigate its extrapolation capability, the trained ANN is then used to predict the fatigue life of three new specimens, and the results are shown in figures 7(C) and (D). It should be noted that the predicted fatigue cycles for each specimen are normalized by their respective predicted fatigue life. As seen in figure 7, the ANN is found to yield accurate fatigue life predictions in LIG interlayered fiberglass composites irrespective of the applied stress magnitude, where the determined R^2 and RMSE corresponding for both training and testing cases are found to be greater than 0.98 and smaller than 10^{-3}, respectively (table S1). Given that the ANN is not bounded by the limitations of conventional numerical models, it is therefore capable of simultaneously describing the various non-linear responses that constitute fatigue damage in fiberglass composites. Consequently, unlike phenomenological models, the ANN makes no assumption regarding the final damage phase of fiber failure and is thus capable of directly learning its characteristic features during the training and validation process.

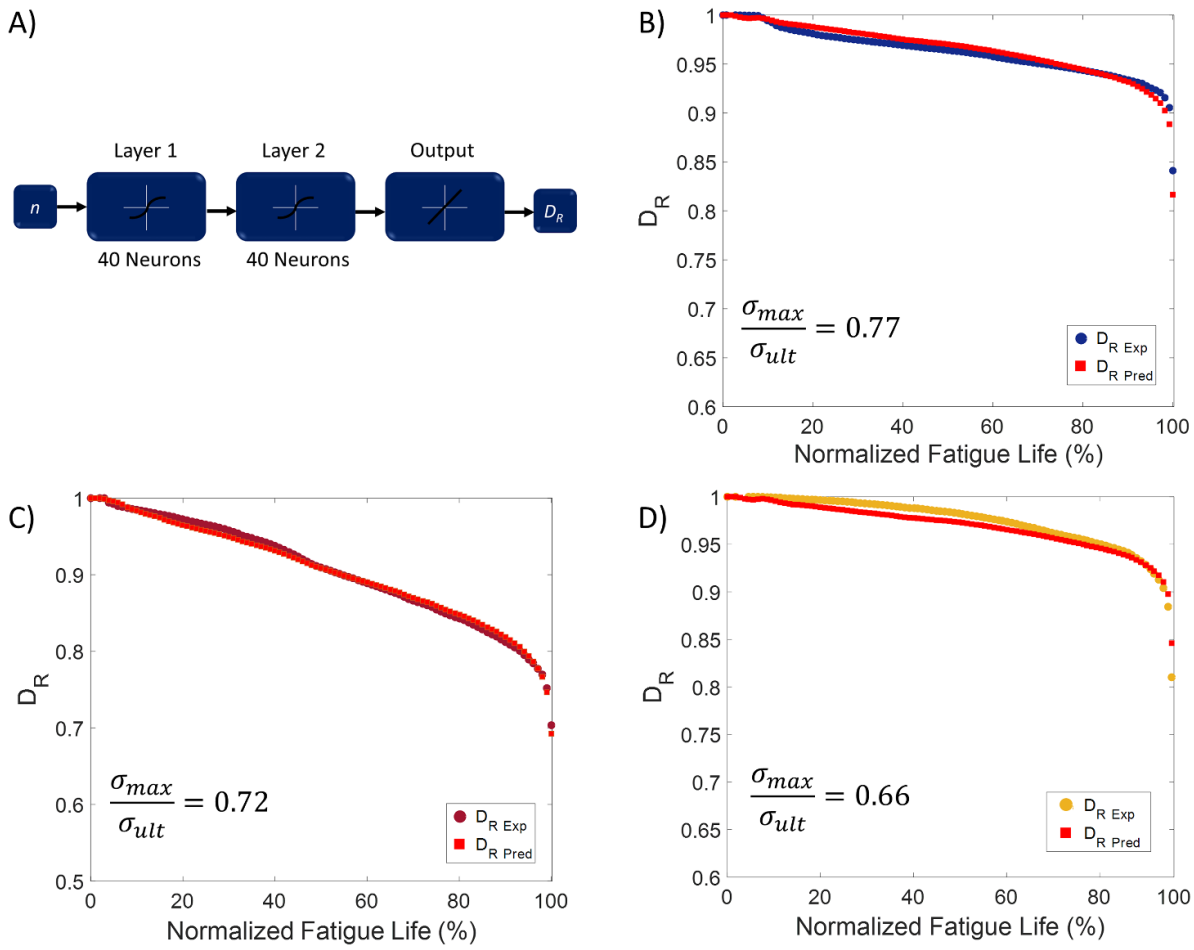

Figure 8. (A) Diagram of used two-layer Bayesian regularized ANN with an optimal number of 40 hidden units or neurons in each layer (ANN_2). (B)–(D) Comparisons between ANN predicted and experimental reduction in the electrical resistance damage parameter (D_R) of LIG interlayered fiberglass composites based on fatigue life cycles and at three different stress levels.

Additionally, such prediction capacity eliminates the need for defining complex failure criterions similar to what was previously discussed in an earlier section, thus considerably simplifying the fatigue life prediction process and greatly improving its accuracy. These claims can be further confirmed by training an ANN in a reverse manner in order to predict D_R in fiberglass specimens when fatigue life cycles are introduced as an input (ANN_2) (figure 8(A)). Again, the trained ANN is tested using three new specimens, and the results are shown in figures 8(B)–(D). The predicted D_R of all three LIG interlayered fiberglass specimens are found to be in good agreement with the experimental results across all three damage phases, as the determined R^2 and RMSE corresponding for both training and testing cases are also found to be greater than 0.98 and smaller than 10^{-3}, respectively (table S1). The ability to predict damage progression over a targeted number of cycles or given an expected fatigue life enables the formulation of closed-loop ANN-based prognosis frameworks that are capable of self-adjusting and improving fatigue life predictions in an iterative manner. Finally, the superior performance of ANNs over degradation phenomenological models can be also validated by examining their corresponding root mean square errors (RMSEs) for both training and validation cases. As seen in table 2, ANN_2 statistically outperforms the phenomenological model and yields more accurate predictions, where 87.6% and 60.4% improvements in RMSE are observed for both training and testing cases, respectively. The performance of the ANN is expected to further enhanced when using a larger and more diverse set of experimental data, such that prediction accuracy can be improved while avoiding overfitting. Evidently, these results confirm the ability of ANN to learn the dynamics governing the degradation in electrical resistance damage parameter D_R due to permanent changes in the piezoresistive response of the LIG interlayers, and to then accurately predict fatigue damage in fiberglass composites according to a specimen-to-specimen scheme.

Table 2. Comparisons of RMSEs for phenomenological and ANN predictions.

	Phenomenological	ANN_2
Training cases	6.21×10^{-4}	3.31×10^{-4}
Tested cases	1.02×10^{-3}	6.34×10^{-4}

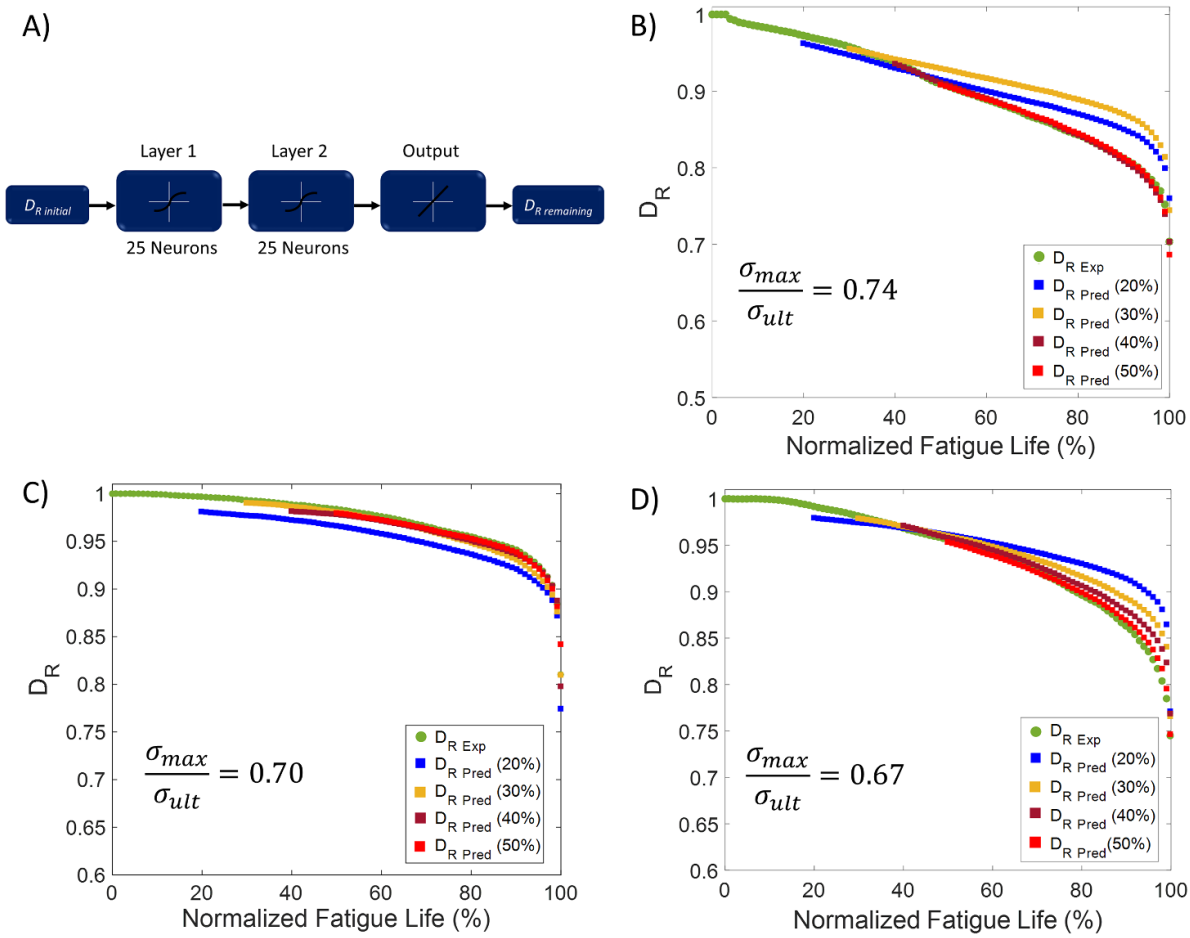

Figure 9. (A) Diagram of used two-layer Bayesian regularized ANNs with an optimal number of 25 hidden units or neurons in each layer (ANN_3-ANN_6). (B)–(D) ANN predictions of reduction in electrical resistance damage parameter (D_R) of LIG interlayered fiberglass composites in a cycle-to-cycle scheme and at three stress levels.

To further evaluate the ability of ANNs to predict changes in D_R based on a cycle-to-cycle scheme, portions of D_R were used as ANN inputs with the goal of predicting future damage progression by solely relying on early stage measurements and observations. Four NNs, ANN_3, ANN_4, ANN_5, and ANN_6 were trained using ten different fiberglass specimens by supplying 20%, 30%, 40%, and 50% of the initial D_R measurements as inputs, respectively. In this case, two-layer Bayesian regularized ANNs with an optimal number of 25 hidden units or neurons in each layer is found to yield the most accurate predictions (figure 9(A)). The trained ANNs are then applied to three new specimens, and as expected, the predictions of future changes in D_R improved with each update, as their accuracy is enhanced with the increasing size of input data (figures 9(B)–(D)). As shown in table S1, R^2 and RMSE corresponding for both training and testing cases when using more than 30% of the initial D_R measurements as inputs are found to be greater than 0.98 and lower than 2×10^{-4}, respectively. As previously described, one of the main advantages of a trained ANN over conventional phenomenological models lies in its ability to accurately predict the final damage phase of fiber breakage up until failure. It should be noted that, in order to eliminate any bias, the ANNs are designed to randomly categorize data sets as training, validation, and testing cases, which explains the reason behind figures 7–9 displaying different fiberglass specimens. Nonetheless, based on these results, it can be confirmed that ANNs are an effective tool for predicting future changes in D_R independent of loading conditions. Future work will aim to incorporate more sophisticated ANN algorithms in order to expand the potential of fatigue life predictions using LIG piezoresistive interlayers, improve their robustness and reliability, while also furthering and easing their integration in real-life structural applications.

4. Conclusion

This study proposes an integrated fatigue damage diagnostics and prognostics procedure for fiberglass composite materials by combining a piezoresistive LIG interlayer-based SHM technique with predictive algorithms such as ANNs and phenomenological models. The LIG interlayered fiberglass composites were subjected to tension–tension fatigue loading while monitoring changes in both their elastic stiffness and

electrical resistances. Damage parameters based on the recorded electrical resistance measurements, D_R and D_{RR}, were defined and their trends were compared to those of conventional stiffness-based ones, D_E and D_{EE}, respectively. The various damage phases and fatigue life of the LIG interlayered fiberglass specimens were then predicted using three non-linear stiffness degradation and damage accumulation models according to electrical resistance-based damage parameters. The predicted responses using the degradation model were found to be largely in good agreement with experimental results, except during the final phase of fatigue life, where fiber failure causes for abrupt and highly non-linear changes in mechanical properties. In the case of both damage accumulation models, the predicted responses were also found to be in good agreement with experimental results, except during the initial phase of matrix cracking due to the relatively low sensitivity of LIG to such a failure mode. Subsequently, ANNs were trained, validated, and then used to yield accurate extrapolations of future fatigue damage progression in LIG interlayered fiberglass specimens, based on both specimen-to-specimen and cycle-to-cycle approaches. Various ANN training algorithms were considered, with BR yielding the most accurate ANN predictions when combined with a network architecture consisting of two hidden layers that contain 40 and 25 neurons in each layer for specimen-to-specimen and cycle-to-cycle schemes, respectively. The ANN predictions were found to be at least 60% more accurate and reliable than those of phenomenological models throughout all damage phases of fatigue life in a specimen-to-specimen scheme, while also requiring less information and being independent of loading conditions. The R^2 and RMSE values of these ANN models were found to be greater than 0.98 and smaller than 10^{-3}, respectively, for both training and testing cases. Similarly, ANN models utilized in a cycle-to-cycle scheme were found to yield accurate predictions of fatigue damage progression once more than 30% of initial D_R measurements are used as inputs, having R^2 and RMSE values greater than 0.99 and smaller than 2×10^{-4}, respectively. Therefore, state-of-the-art ANN architectures can be coupled with piezoresistive LIG-based SHM methods to continuously and accurately update fatigue damage predictions in composite materials. Future work will aim to further expand on such techniques to allow for simple, contactless, and reliable predictions of fatigue phenomena in composite structures used in dynamic engineering systems.

Data availability statement

The data that support the findings of this study are available upon reasonable request from the authors.

Acknowledgments

This work was supported by the National Science Foundation Grants # CMMI-1762369 and # EFRI-1935216, and the Air Force Office of Scientific Research under Grant # FA9550-16-1-0087.

ORCID iDs

Jalal Nasser https://orcid.org/0000-0002-0898-3801
LoriAnne Groo https://orcid.org/0000-0001-5296-1354
Henry Sodano https://orcid.org/0000-0001-6269-1802

References

[1] Kim J-K and Mai Y W 1998 *Engineered Interfaces in Fiber Reinforced Composites* (Oxford,UK: Elsevier Sciences)
[2] Chawla K K 2012 *Composite Materials: Science and Engineering* (Berlin: Springer)
[3] Gibson R F 2016 *Principles of Composite Material Mechanics* (Boca Raton, FL: CRC Press)
[4] Sohn H, Farrar C R, Hemez F M and CZarnecki J J 2002 A review of structural health review of structural health monitoring literature 1996–2001 *OSTI.GOV Third World Conf. on Structural Control* (*Como*)
[5] Montalvão D, Maia N M M and Ribeiro A M R 2006 A review of vibration-based structural health monitoring with special emphasis on composite materials *Shock Vib. Dig.* **38** 295–324
[6] Talreja R 2003 *Fatigue of Composite Materials* (Berlin: Springer)
[7] Krause T, Preihs S and Ostermann J 2015 Acoustic emission damage detection for wind turbine rotor blades using airborne sound *Structural Health Monitoring* (Stanford, CA: DEStech Publications) 340–7
[8] Hamstad M A 1986 A review: acoustic emission, a tool for composite-materials studies *Exp. Mech.* **26** 7–13
[9] Barré S and Benzeggagh M L 1994 On the use of acoustic emission to investigate damage mechanisms in glass-fibre-reinforced polypropylene *Compos. Sci. Technol.* **52** 369–76
[10] Read I, Foote P and Murray S 2002 Optical fibre acoustic emission sensor for damage detection in carbon fibre composite structures *Meas. Sci. Technol.* **13** 5–9
[11] Wu Q, Yu F, Okabe Y and Kobayashi S 2015 Application of a novel optical fiber sensor to detection of acoustic emissions by various damages in CFRP laminates *Smart Mater. Struct.* **24** 015011
[12] Gao S, Zhuang R-C, Zhang J, Liu J-W and Mäder E 2010 Glass fibers with carbon nanotube networks as multifunctional sensors *Adv. Funct. Mater.* **20** 1885–93
[13] Böger L, Wichmann M H G, Meyer L O and Schulte K 2008 Load and health monitoring in glass fibre reinforced composites with an electrically conductive nanocomposite epoxy matrix *Compos. Sci. Technol.* **68** 1886–94
[14] Wang S and Chung D D L 2006 Self-sensing of flexural strain and damage in carbon fiber polymer-matrix composite by electrical resistance measurement *Carbon* **44** 2739–51
[15] Wang S, Chung D D L and Chung J H 2005 Impact damage of carbon fiber polymer-matrix composites, studied by electrical resistance measurement *Composites* A **36** 1707–15
[16] Schulte K and Baron C 1989 Load and failure analyses of CFRP laminates by means of electrical resistivity measurements *Compos. Sci. Technol.* **36** 63–76
[17] Balberg I 2002 A comprehensive picture of the electrical phenomena in carbon black-polymer composites *Carbon* **40** 139–43
[18] Tallman T N, Gungor S, Wang K W and Bakis C E 2015 Damage detection via electrical impedance tomography in glass fiber/epoxy laminates with carbon black filler *Struct. Heal. Monit.* **14** 100–9
[19] Baltopoulos A, Polydorides N, Pambaguian L, Vavouliotis A and Kostopoulos V 2015 Exploiting carbon nanotube

networks for damage assessment of fiber reinforced composites *Composites* B **76** 149–58
[20] Zhang J, Zhuang R, Liu J, Mäder E, Heinrich G and Gao S 2010 Functional interphases with multi-walled carbon nanotubes in glass fibre/epoxy composites *Carbon* **48** 2273–81
[21] Alexopoulos N D, Bartholome C, Poulin P and Marioli-Riga Z 2010 Structural health monitoring of glass fiber reinforced composites using embedded carbon nanotube (CNT) fibers *Compos. Sci. Technol.* **70** 260–71
[22] Nofar M, Hoa S V and Pugh M D 2009 Failure detection and monitoring in polymer matrix composites subjected to static and dynamic loads using carbon nanotube networks *Compos. Sci. Technol.* **69** 1599–606
[23] Gao L, Thostenson E T, Zhang Z and Chou T-W 2009 Sensing of damage mechanisms in fiber-reinforced composites under cyclic loading using carbon nanotubes *Adv. Funct. Mater.* **19** 123–30
[24] Parmar K, Mahmoodi M, Park C and Park S S 2013 Effect of CNT alignment on the strain sensing capability of carbon nanotube composites *Smart Mater. Struct.* **22** 075006
[25] Gojny F H, Wichmann M H G, Köpke U, Fiedler B and Schulte K 2004 Carbon nanotube-reinforced epoxy-composites: enhanced stiffness and fracture toughness at low nanotube content *Compos. Sci. Technol.* **64** 2363–71
[26] An Q, Rider A N and Thostenson E T 2012 Electrophoretic deposition of carbon nanotubes onto carbon-fiber fabric for production of carbon/epoxy composites with improved mechanical properties *Carbon* **50** 4130–43
[27] Bekyarova E, Thostenson E T, Yu A, Kim H, Gao J, Tang J, Hahn H T, Chou T-W, Itkis M E and Haddon R C 2007 Multiscale carbon nanotube−carbon fiber reinforcement for advanced epoxy composites *Langmuir* **23** 3970–4
[28] Steinke K, Groo L A and Sodano H A 2021 Laser induced graphene for *in-situ* ballistic impact damage and delamination detection in aramid fiber reinforced composites *Compos. Sci. Technol.* **202** 108551
[29] Groo L A, Nasser J, Inman D and Sodano H 2021 Laser induced graphene for *in situ* damage sensing in aramid fiber reinforced composites *Compos. Sci. Technol.* **201** 108541
[30] Groo L A, Nasser J, Zhang L, Steinke K, Inman D and Sodano H 2020 Laser induced graphene in fiberglass-reinforced composites for strain and damage sensing *Compos. Sci. Technol.* **199** 108367
[31] Groo L, Nasser J, Inman D and Sodano H 2021 Damage localization in fiberglass-reinforced composites using laser induced graphene *Smart Mater. Struct.* **30** 035006
[32] Lin J, Peng Z, Liu Y, Ruiz-Zepeda F, Ye R, Samuel E L G, Yacaman M J, Yakobson B I and Tour J M 2014 Laser-induced porous graphene films from commercial polymers *Nat. Commun.* **5** 5714
[33] Duy L X, Peng Z, Li Y, Zhang J, Ji Y and Tour J M 2018 Laser-induced graphene fibers *Carbon* **126** 472–9
[34] Groo L A, Nasser J, Inman D and Sodano H 2021 Fatigue damage tracking and life prediction of fiberglass composites using a laser induced graphene interlayer *Composites* B **218** 108935
[35] Kashtalyan M and Soutis C 2000 Stiffness degradation in cross-ply laminates damaged by transverse cracking and splitting *Composites* A **31** 335–51
[36] Taheri-Behrooz F, Shokrieh M M and Lessard L B 2008 Residual stiffness in cross-ply laminates subjected to cyclic loading *Compos. Struct.* **85** 205–12
[37] Whitworth H A 1997 A stiffness degradation model for composite laminates under fatigue loading *Compos. Struct.* **40** 95–101
[38] Owen M J and Howe R J 1972 The accumulation of damage in a glass-reinforced plastic under tensile and fatigue loading *J. Phys. D: Appl. Phys.* **5** 1637–49
[39] Wilkins E W C 1956 *Cumulative Damage in Fatigue* (Berlin: Springer)
[40] Suzuki T, Mahfuz H and Takanashi M 2019 A new stiffness degradation model for fatigue life prediction of GFRPs under random loading *Int. J. Fatigue* **119** 220–8
[41] Wu F and Yao W X 2010 A fatigue damage model of composite materials *Int. J. Fatigue* **32** 134–8
[42] Subramanian S, Reifsnider K L and Stinchcomb W W 1995 A cumulative damage model to predict the fatigue life of composite laminates including the effect of a fibre-matrix interphase *Int. J. Fatigue* **17** 343–51
[43] Yang J N, Lee L J and Sheu D Y 1992 Modulus reduction and fatigue damage of matrix dominated composite laminates *Compos. Struct.* **21** 91–100
[44] Zhang W, Ma J, Gao L, Zhang Z and Gao H 2015 Fatigue life and resistance analysis of COG assemblies under hygrothermal aging *Microelectron. Reliab.* **55** 623–9
[45] Shiri S, Yazdani M and Pourgol-Mohammad M 2015 A fatigue damage accumulation model based on stiffness degradation of composite materials *Mater. Des.* **88** 1290–5
[46] Eser A, Aşkar Ayyildiz E, Ayyildiz M and Kara F 2021 Artificial intelligence-based surface roughness estimation modelling for milling of AA6061 alloy *Adv. Mater. Sci. Eng.* **2021** 1–10
[47] Kara F, Karabatak M, Ayyildiz M and Nas E 2020 Effect of machinability, microstructure and hardness of deep cryogenic treatment in hard turning of AISI D2 steel with ceramic cutting *J. Mater. Res. Technol.* **9** 969–83
[48] Ö E, Işık B, Çiçek A and Kara F 2013 Prediction of damage factor in end milling of glass fibre reinforced plastic composites using artificial neural network *Appl. Compos. Mater.* **20** 517–36
[49] Karnik S R, Gaitonde V N, Rubio J C, Correia A E, Abrão A M and Davim J P 2008 Delamination analysis in high speed drilling of carbon fiber reinforced plastics (CFRP) using artificial neural network model *Mater. Des.* **29** 1768–76
[50] Al-Haik M S, Hussaini M Y and Garmestani H 2006 Prediction of nonlinear viscoelastic behavior of polymeric composites using an artificial neural network *Int. J. Plast.* **22** 1367–92
[51] Vassilopoulos A P 2020 *Fatigue Life Prediction of Composites and Composite Structures* (Amsterdam: Elsevier)
[52] Al-Assaf Y and El Kadi H 2007 Fatigue life prediction of composite materials using polynomial classifiers and recurrent neural networks *Compos. Struct.* **77** 561–9
[53] Genel K 2004 Application of artificial neural network for predicting strain-life fatigue properties of steels on the basis of tensile tests *Int. J. Fatigue* **26** 1027–35
[54] Tao C, Zhang C, Ji H and Qiu J 2021 Application of neural network to model stiffness degradation for composite laminates under cyclic loadings *Compos. Sci. Technol.* **203** 108573
[55] Zhang C, Zhang Z, Ji H, Qiu J and Tao C 2020 Mode conversion behavior of guided wave in glass fiber reinforced polymer with fatigue damage accumulation *Compos. Sci. Technol.* **192** 108073
[56] Peng T, Liu Y, Saxena A and Goebel K 2015 *In-situ* fatigue life prognosis for composite laminates based on stiffness degradation *Compos. Struct.* **132** 155–65
[57] Seo D C and Lee J J 1999 Damage detection of CFRP laminates using electrical resistance measurement and neural network *Compos. Struct.* **47** 525–30
[58] Nasser J, Zhang L and Sodano H 2021 Laser induced graphene interlaminar reinforcement for tough carbon fiber/epoxy composites *Compos. Sci. Technol.* **201** 108493

[59] Nasser J, Groo L A, Zhang L and Sodano H 2020 Laser induced graphene fibers for multifunctional aramid fiber reinforced composite *Carbon* **158** 146–56
[60] Cytec 2011 *CYCOM ® E773 Epoxy Prepreg-Technical Data Sheet*
[61] Çay Y, Çiçek A, Kara F and Sağiroğlu S 2012 Prediction of engine performance for an alternative fuel using artificial neural network *Appl. Therm. Eng.* **37** 217–25
[62] Kayri M 2016 Predictive abilities of Bayesian regularization and Levenberg–Marquardt algorithms in artificial neural networks: a comparative empirical study on social data *Math. Comput. Appl.* **21** 20
[63] Reifsnider K L 2012 *Fatigue of Composite Materials—Google Books* vol 4, ed R B Pipes (Amsterdam: Elsevier)
[64] Yang J N, Jones D L, Yang S H and Meskini A 1990 A stiffness degradation model for graphite/epoxy laminates *J. Compos. Mater.* **24** 753–69
[65] Yang J N, Yang S H and Jones D L 1989 Stiffness-based statistical model for predicting the fatigue life of graphite/epoxy laminates *J. Compos. Technol. Res.* **11** 129–34